Semi–autonomous exploration of multi–floor buildings with a legged robot

Garrett J. Wenger[a], Aaron M. Johnson[b], Camillo J. Taylor[c], and Daniel E. Koditschek[a]

[a]Electrical & Systems Engineering, University of Pennsylvania, Philadelphia, PA
[b]Robotics Institute, Carnegie Mellon University, Pittsburgh, PA
[c]Computer & Information Science, University of Pennsylvania, Philadelphia, PA

ABSTRACT

This paper presents preliminary results of a semi-autonomous building exploration behavior using the hexapedal robot RHex. Stairwells are used in virtually all multi-floor buildings, and so in order for a mobile robot to effectively explore, map, clear, monitor, or patrol such buildings it must be able to ascend and descend stairwells. However most conventional mobile robots based on a wheeled platform are unable to traverse stairwells, motivating use of the more mobile legged machine. This semi-autonomous behavior uses a human driver to provide steering input to the robot, as would be the case in, e.g., a tele-operated building exploration mission. The gait selection and transitions between the walking and stair climbing gaits are entirely autonomous. This implementation uses an RGBD camera for stair acquisition, which offers several advantages over a previously documented detector based on a laser range finder, including significantly reduced acquisition time. The sensor package used here also allows for considerable expansion of this behavior. For example, complete automation of the building exploration task driven by a mapping algorithm and higher level planner is presently under development.

Keywords: autonomy, stair climbing, hexapod, gait selection

1. INTRODUCTION

This paper documents experiments with a guarded exploration behavior dealing primarily with automated gait selection driven by a robust vision-based stairwell detector. The behavior is been implemented on the X-RHex[1] version of the RHex[2] platform, which offers a longer possible runtime and greater payload carrying capacity than other RHex variants. The sensor payload used for these experiments consists of an RGBD Camera*, an IMU†, and an additional computer‡ to supplement the one onboard.

Urban search and rescue (USAR) and intelligence, surveillance, reconnaissance (ISR) tasks are well established applications of teleoperated mobile robots. Whereas full autonomy is not always needed, the benefits of 'human-in-the-loop' control[3] rely upon a lower level of sensorimotor autonomy, which is required to eliminate the need for operator skill and prior training with the robotic platform,[4] and to free attention for focus on the intrinsic requirements of the task. In the setting of this paper, gait selection and transition control are automated so that the operator's experience is more similar to driving an RC car, obviating any need for familiarity with body and leg kinematics and dynamics.

The sensor used here offers many advantages over a previous implementation which utilized a laser scanner.[5] The RGBD camera returns 2D images, eliminating the need for the 'pitch wiggle'[6,7] used along with the LIDAR sensor. This greatly decreases the time it takes to find stairs, since the 'pitch wiggle' can only be executed while RHex is stationary. Such 'while-navigating' autonomy enables more seamless interactions between robot and operator than were possible before, and it has been implemented in a way that is platform agnostic, allowing for simple adaptations to other robots. A conventional digital camera could also be used to enable this sort of autonomy,[8] but the RGBD camera should allow for better stair detection in poorly lit environments, which can be expected during building exploration tasks.

*ASUS XTion PRO Camera `http://www.asus.com/Multimedia/Xtion_PRO/`
†Microstrain 3DM-GX3-25 IMU `http://www.microstrain.com/inertial/3DM-GX3-25`
‡Apple Mac Mini `https://www.apple.com/mac-mini/`

2. DESCRIPTION OF SEMI–AUTONOMOUS BEHAVIOR

The behavior presented here consists of three distinct parts: the stair detector, the semi–autonomous gait selector, and the stair climbing transition and gait,[5,9,10] which have been described previously. All computing is done on either the payload computer or robot computer itself. The equipment setup used to run this behavior is shown in Fig. 1, and the mass breakdown is listed in Table 1. This behavior requires a human operator to guide the robot when away from stairs and on landings (whence the "semi–autonomous" title).

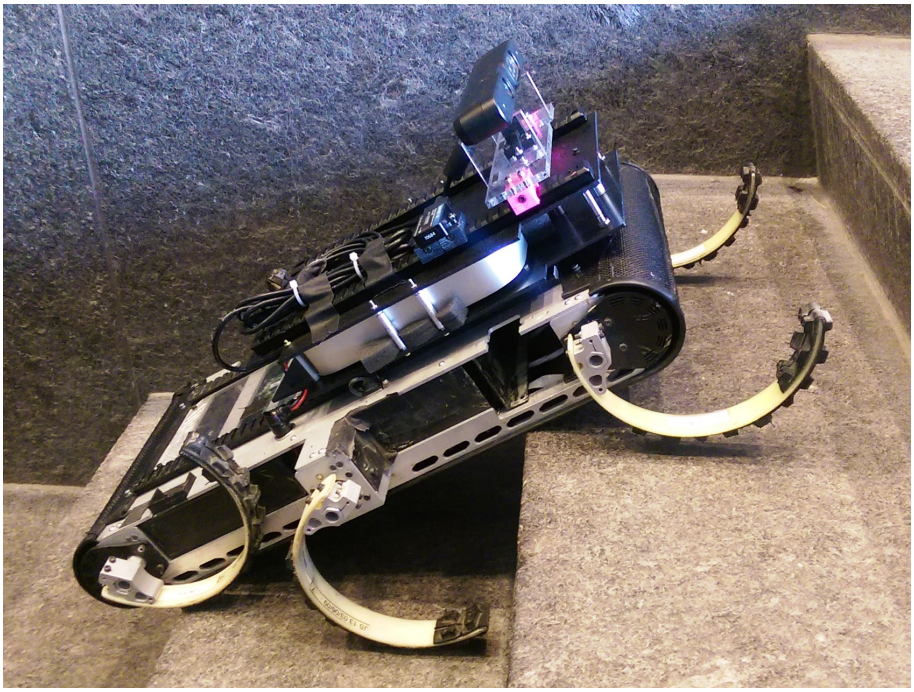

Figure 1. RHex displaying its payload (Mac Mini, RGBD camera, IMU) while climbing

Table 1. Mass of the robot and its payload

X-RHex + 1 battery	9.057 kg
Mac Mini (w/ mount)	1.897 kg
RGBD camera (w/ mount)	.325 kg
IMU	.052 kg
Total mass	**11.327 kg**

2.1 Stair detection algorithm

The first goal of the stair detection procedure is to determine whether a staircase appears in a given RGBD image acquired by the robot. If a staircase is detected the detector must return estimates for the position and orientation of the start of the staircase along with the rise and run of the steps.

Fig. 2 shows an RGBD image acquired an ASUS Xtion sensor mounted on the robot; in this case the frame contains a staircase which the system must detect and localize. In the experimental setup the optical axis of the depth camera was approximately parallel to the ground plane. This allows ready extraction of feature points in the depth frame that correspond to vertical surfaces like walls and stair risers by considering the surface normals in the depth image.

Once the vertical surface elements have been identified the second phase of the analysis procedure seeks to estimate the dominant rectilinear structure of the scene. This can be done by employing the entropy compass idea described in [11, Section II]. Consider the 2D point set obtained by projecting all of the vertical surface

Figure 2. Example RGBD frame containing a staircase.

elements onto the ground plane, then rotate this set of points around the vertical axis in 1 degree increments, and for each such yaw angle compute the entropy of the X and Y coordinates. When plotting the sum of these entropies as a function of angle, the global minimum reliably corresponds to the dominant orientation of the structure. The detection algorithm extracts this angle and uses it to automatically produce axis aligned coordinates as shown in Fig. 3. Note that the lines inscribed on this figure correspond to salient axis-aligned surfaces that are automatically discovered by the system. In this case these surfaces correspond to the stair risers, the supporting wall and the staircase banister. Note that in this figure the stair risers and the walls are aligned with the X and Y axes which simplifies subsequent analysis.

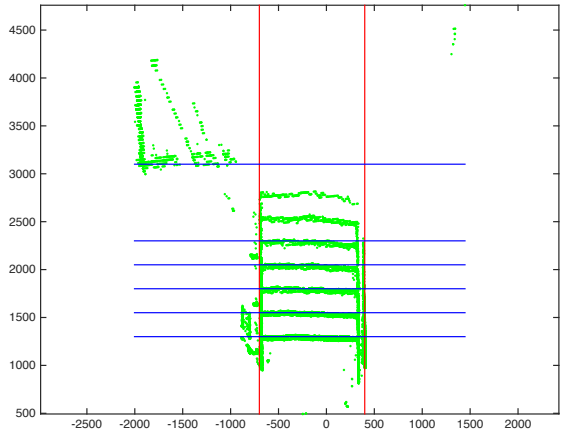

Figure 3. This figure shows an overhead view of the scene after the axis alignment procedure. Note that the salient vertical surfaces, the walls and the stair risers are now aligned with the x and y axes which simplifies subsequent analysis.

To detect stair patterns, the algorithm considers each column of the image in turn. Fig. 4 shows a plot of the depth values as a function of row index for one such column in the middle of the image. Notice that this particular column exhibits a canonical pattern corresponding to a staircase where the depth values change in a predictable pattern as the row index increases. The analysis procedure considers the derivative of this signal and seeks to identify a set of regularly spaced spikes corresponding to the stair edges. If it finds a sequence of 3 or more such stair edges it decides that the image contains a staircase. The magnitude and spacing of the discontinuities in the depth profile are used to calculate the rise and run of the steps. These measurements are currently only used to reject structures which have stair-like features but are outside of typical stair sizes.

Once a staircase has been detected in the image the system tries to find significant wall surfaces that are perpendicular to the detected stair risers and constrain the width of the staircase. In Fig. 3 the red lines indicate the two surfaces that the system discovered for this example staircase image.

Note that since the entropy compass procedure produces an angle, the robot is able to gauge its position and

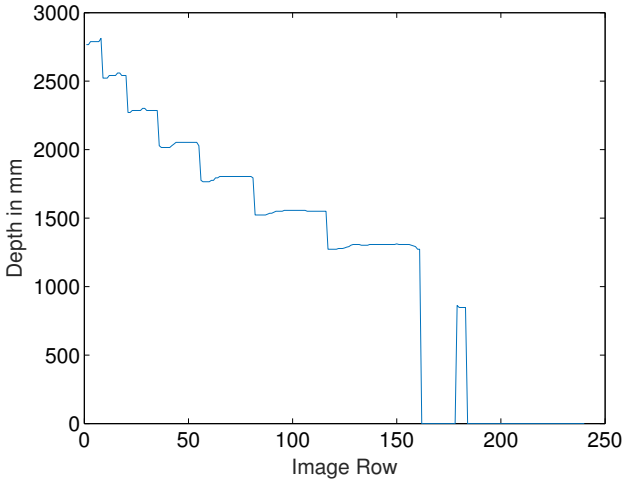

Figure 4. This figure shows how the depth varies as a function of row index for one of the columns in the middle of the image. Note the characteristic stair case pattern which the code seeks to detect.

orientation relative to the staircase, and these estimates are used in the control procedure to guide the robot to a suitable starting point to begin its climb.

Table 2 shows the current performance of the detector based on measurements of the rise and run of a set of stairs. All of the measurements are slightly lower than the ground truth, and there is some variation based on the sensor's position.

Table 2. Stair measurements, robot measurements calculated from depth camera

Measurement method	Rise (cm)	Run (cm)
Ground truth	18.0	28.0
Robot sitting, 1.15m from 1st step	16.2	26.2
Robot standing, 1.15m from 1st step	15.5	26.0
Robot sitting, .5m from 1st step	15.5	26.8
Robot standing, .5m from 1st step	16.0	27.0

2.2 Semi–autonomous gait selection

The gait selection behavior runs directly on the robot computer, as an operator provides speed and steering inputs using a joystick over a wireless connection. While RHex is driven around, the gait selector polls the stair detector at a frequency of about 1 Hz. The actual detection algorithm completes much more quickly than this, but this rate was found to be generally sufficient at walking speeds through cluttered environments. When a set of stairs is in view, the gait selection behavior checks the robot's distance from the first stair and angle with respect to the axis of the flight of steps. If the distance and angle are within a predetermined range of acceptable values, the gait selector activates the stair gait transition [10, Section IV.A], and user control is disabled. This range of values was determined by manually activating the stair climbing gait with RHex at various distances and angles from a set of stairs and observing which initial conditions allowed for reliably successful transitions onto the first step. While climbing, the camera is not used, but it would be suitable for obstacle detection and mapping. When the robot determines that it has reached a landing based on readings from its IMU [5, Section III.B.1], navigational control returns to the operator and the selector re-enables the stair detection algorithm.

3. METHODS AND RESULTS

The semi–autonomous behavior was tested on a variety of stairwells around the University of Pennsylvania and Fort Indiantown Gap, Range 30[§]. A trial consists of a simulated building exploration task, wherein the operator steers RHex around open areas, rooms, and landings as well as stairwells. On each floor, the operator again explores the surrounding areas before returning to the stairwell. For this reason, the trial times listed in Table 3 are much longer than they would be if the goal of these tests was to reach the top floor as quickly as possible. As a comparison, note that while the stair A and D trials cover the same number of steps, the stair D trials were completed much faster because there were no open areas to traverse between flights.

We attempted to find stairwells with varied features to test the behavior. Stairwells A and B (which had identical steps, but different landings and steps per flight) were made of extremely smooth concrete and each step had a rounded nose. These were also steepest steps used in these tests. For these reasons, RHex slipped while executing the stair climbing gait (that is, the robot slid back about half a step before recovering and continuing to climb) rather frequently. The total number of slips has been listed for each of the 6 trials. All of the other stairwells had sharp noses, and the construction materials (stone, unpolished cement, rough tread) offer a higher coefficient of friction. Fig. 5 shows the collection of stairs used during the trials.

Figure 5. Stairs used to test the semi–autonomous behavior

Overall, the robot climbed 76 flights totaling 713 steps with only 6 climbing failures (of which 2 were recovered from without operator intervention). Out of the 76 flights, there were separate 3 instances where the behavior failed to activate the stair climbing transition in time, and all of these instances occurred after making a very tight turn. This issue could likely be fixed by slightly increasing the sampling rate of the detection algorithm. Between climbing and behavior failures, RHex faulted on 11.8% (9/76) of all flights climbed. Apart from those two failure areas, RHex slipped on 3.7% (26/713) of all steps or 10.4% (26/249) of steps in stairwells A and B. Slipping is not considered a failure for these experiments because it did halt the robot's progress. It is also worth noting that all of the stairwell C and D trials were conducted during one 55 minute period when the robot and payload were continuously powered by a single battery. The X-RHex variation of the RHex platform is capable of carrying two batteries at a time, so this robot and behavior should be suitable for the execution of lengthy tasks.

Throughout several hours of testing in environments with typical building clutter (e.g. desks, chairs, pillars), the only false positive stair detection occurred outside of normal use when the camera was turned on its side and held at a shallow angle with respect to a set of parallel bars. This implies that horizontal bars on the ground (e.g. a sewer grate) could potentially cause a false positive, however this source of error has since been mitigated

[§]`http://ftig.ng.mil/training/Pages/default.aspx`

Table 3. Results from 15 trials of the semi–autonomous behavior. The number of steps per flight varied within a trial, and so those numbers are not shown here. Instead the number of flights is given to provide a measure of the stair detector's success (with 76 total flights climbed), and the number of stairs per trial is shown to emphasize the robot's endurance (total of 713 stairs climbed over 98:24 minutes). This behavior is relatively capable of ignoring the specific structure of a stairwell; stair E has the minimum slope of 0.53, and stairs A&B have the maximum slope of 0.64.

Trial	Rise (cm)	Run (cm)	Flights	Stairs	Time (mm:ss)	Notes
Stair A-1	18.0	28.0	9	63	12:17	Transition onto first step failed once, behavior automatically reacquired stairs and was successful on second attempt, 8 slips
Stair A-2	18.0	28.0	9	63	12:09	Robot scraped along wall for one flight of stairs due to poor steering (operator error), behavior successful regardless, 8 slips
Stair A-3	18.0	28.0	9	63	13:45	Transition out of stair climbing stalled once, walking phase activated manually, 4 slips
Stair B-1	18.0	28.0	2	20	5:20	One stair detection failure due to sensor timing after making a sharp turn, one transition failure where RHex nearly walked off open edge of stairwell, 2 slips
Stair B-2	18.0	28.0	2	20	3:50	Route avoided sharp turn, no faults, 0 slips
Stair B-3	18.0	28.0	2	20	3:30	Same route as in B-1, no faults, 4 slips
Stair C-1	17.3	31.6	2	27	3:39	Flipped on transition to 3rd flight, smashed camera mount and ended trial
Stair C-2	17.3	31.6	4	55	5:48	Broke rear left leg climbing final step, trial succeeded regardless
Stair C-3	17.3	31.6	4	55	5:32	Nearly pitched back during one transition, operator intervened to prevent damage
Stair D-1	17.4	30.9	6	63	5:19	Detector twice missed stairs after rounding a sharp corner, operator reset on landing and behavior continued successfully
Stair D-2	17.4	30.9	6	63	4:54	No faults
Stair D-3	17.4	30.9	6	63	5:16	Transition onto first step failed once, behavior automatically reacquired stairs and was successful on second attempt
Stair E-1	16.8	31.8	5	46	5:44	No faults
Stair E-2	16.8	31.8	5	46	5:51	No faults
Stair E-3	16.8	31.8	5	46	5:30	No faults

by ignoring 'stairs' where the step sizes as returned by the detection algorithm are outside of an expected range. Other than this single forced instance, there were no false positive detections during any of the trials.

An additional set of trials was conducted to examine the sensitivity of the semi–autonomous behavior to the mass distribution of the robot and payload. For these trials, RHex transitions to the stair climbing gait and climbs three steps of a stair C flight. Only three steps are used because any transition failures happened during the transition itself or on the first step after the transition. X-RHex's payload position and battery configuration (single battery in front, single battery in back, both batteries) were varied, with each setup being tested 20 times. A summary of these trials is presented in Table 4. With the COM positioned behind the center of the robot, RHex failed to transition onto the stairs 64% (90/140) of the time. Otherwise, the robot only failed on 3% (5/160) of all attempts. However, the front battery/-12 cm and both battery/-6 cm configurations had very similar COM positions, but significantly different failure rates (65% vs 15%). Thus the success of the gait transition is highly dependent on not just the location of the robot's center of mass (COM) but also on the actual weight distribution of the robot and payload. All of the exploration trials (Table 3) were performed in the front battery/+12 cm configuration.

Table 4. Summary of COM effect on transition failure rate. Positions are measured in cm from the center of the robot frame, which coincides with its COM when no payload is installed and both battery bays are full (or empty). Specifically, the payload position is the forward displacement of the payload mount's midpoint with respect to the robot's center. The vertical displacement of the COM is +1.47 cm with both batteries installed or +1.61 cm with a single battery. Each configuration was tested 20 times (300 total trials).

Payload	Front battery					Both batteries					Rear battery				
position	-12	-6	0	+6	+12	-12	-6	0	+6	+12	-12	-6	0	+6	+12
COM pos	-1.0	+0.2	+1.4	+2.6	+3.8	-2.2	-1.1	0	+1.1	+2.2	-3.8	-2.6	-1.4	-0.2	+1.0
Failures	13	0	0	1	1	17	3	1	0	1	20	18	17	2	1

4. CONCLUSION AND FUTURE WORK

We have demonstrated success of a limited semi–autonomous exploration behavior using a camera sensor which allows for significant future expansion. In the current setup, stair acquisition can be performed without needing to stop and process the robot's surroundings. With the previous sensor, this type of 'mobile' autonomy would not be possible. The camera also allows for the creation of more detailed maps than are possible with the LIDAR. Thus the new sensor morphology has enabled investigation of an enhanced level of autonomy, and this behavior is the first step towards further abstraction of the robot's dynamics from a teleoperator or even possibly full autonomy.

The practical utility of this behavior in the targeted application scenarios awaits the addition of a stair descent controller,[9] as well as more sophisticated navigational capabilities (such as mapping, localization and obstacle avoidance), all of which are achievable with the current payload. As shown, the stair gait transition is prone to failure based on the location of the payload. To increase the reliability of the transition, and hence the usability of the behavior, the stair climbing gait will be reworked to account for pitch control (informed by the sensor's stair dimension estimates) while climbing rather than relying on the present fixed gait. The stair detector's performance deteriorates as the camera gets washed out by sunlight, so it typically only works indoors or in shadow — and any surfaces that reflect IR light are likely to degrade its performance. The detection algorithm also does not currently work on stairs with open risers. The light and reflectance sensitivity will always be problematic with this choice of sensor, but the restrictive geometric assumptions can likely be improved upon with future updates to the detector.

ACKNOWLEDGMENTS

This work was supported by the ARL/GDRS RCTA project, Coop. Agreement #W911NF-10-2-0016.

REFERENCES

[1] Galloway, K. C., Haynes, G. C., Ilhan, B. D., Johnson, A. M., Knopf, R., Lynch, G., Plotnick, B., White, M., and Koditschek, D. E., "X-RHex: A highly mobile hexapedal robot for sensorimotor tasks," tech. rep., University of Pennsylvania (2010).

[2] Saranli, U., Buehler, M., and Koditschek, D. E., "RHex: A simple and highly mobile hexapod robot," *International Journal of Robotics Research* **20**(7), 616–631 (2001).

[3] Murphy, R. and Burke, J., "From remote tool to shared roles," *Robotics Automation Magazine, IEEE* **15**, 39–49 (Dec 2008).

[4] Pratt, K. and Murphy, R., "Protection from human error: Guarded motion methodologies for mobile robots," *Robotics Automation Magazine, IEEE* **19**, 36–47 (Dec 2012).

[5] Johnson, A. M., Hale, M. T., Haynes, G. C., and Koditschek, D. E., "Autonomous legged hill and stairwell ascent," in [*IEEE International Workshop on Safety, Security, & Rescue Robotics, SSRR*], 134–142 (November 2011).

[6] Sayginer, E., Akbey, T., Yazicioglu, Y., and Saranli, A., "Task oriented kinematic analysis for a legged robot with half-circular leg morphology," in [*Robotics and Automation, 2009. ICRA '09. IEEE International Conference on*], 4088–4093 (May 2009).

[7] Johnson, A. M. and Koditschek, D. E., "Legged self-manipulation," *IEEE Access* **1**, 310–334 (May 2013).

[8] Mourikis, A. I., Trawny, N., Roumeliotis, S. I., Helmick, D. M., and Matthies, L., "Autonomous stair climbing for tracked vehicles," *The International Journal of Robotics Research* **26**(7), 737–758 (2007).

[9] Moore, E., Campbell, D., Grimminger, F., and Buehler, M., "Reliable stair climbing in the simple hexapod 'RHex'," in [*Robotics and Automation, 2002. Proceedings. ICRA'02. IEEE International Conference on*], **3**, 2222–2227, IEEE (2002).

[10] Haynes, G. C. and Rizzi, A. A., "Gaits and gait transitions for legged robots," in [*Proceedings of the IEEE International Conference On Robotics and Automation*], 1117–22 (May 2006).

[11] Cowley, A., Taylor, C. J., and Southall, B., "Rapid multi-robot exploration with topometric maps," in [*Proc. IEEE International Conference on Robotics and Automation (ICRA)*], (2010).